Desalination and Water Treatment
www.deswater.com

doi: 10.5004/dwt.2017.21524

95 (2017) 227–233
November

Different types of biochar: effect of aging on the Cu(II) adsorption behavior

Hao Hao[a,b], Yan-de Jing[a,b,*], Wen-liang Ju[a,b], Lei Shen[a,b], Yong-qiang Cao[a,b]

[a] *Key Laboratory of Nansi Lake Wetland Ecological and Environmental Protection in Universities of Shandong, Jining, Shandong 273165, China, emails: jingyande@163.com (Y.-d. Jing), 783653538@qq.com (H. Hao), 1036910764@qq.com (W.-l. Ju), 961617375@qq.com (L. Shen), 1319901868@qq.com (Y.-q. Cao)*
[b] *College of Geography and Tourism, Qufu Normal University, Rizhao, Shandong 276826, China*

Received 9 August 2017; Accepted 4 October 2017

ABSTRACT

Biochar has been recognized as an effective heavy metal adsorbent; however, there is limited knowledge on the effect of biochar aging on its heavy metal adsorption behavior. To study the effect of aging on the Cu(II) adsorption behavior of different biochar types, the surface properties and adsorption characteristics of peanut biochar (PB), cotton biochar (CB) and their corresponding dry-wet aging biochar (PDB, CDB) were analyzed. After the dry-wet aging process, the Cu(II) adsorption capacity of cotton-derived biochar was increased by 292%, whereas the Cu(II) adsorption capacity of peanut-derived biochar decreased by 45.56%. At the same time, the O/C ratio of the two biochar types increased, and the increase for CB was more considerable than that for PB. Considering that there was a consistency between the changes of the specific surface area, ash content and adsorption capacity of the biochar, we inferred that the change of specific surface area and ash content of biochar may be the main reasons for the change of adsorption capacity.

Keywords: Biochar; Aging; Cu(II); Adsorption

1. Introduction

With the industrial process accelerating, copper pesticide excessive application makes the water and soil copper pollution more and more serious, and a large number of copper ions are released into surface and underground water, which directly or indirectly harms human health. According to statistics, the annual emissions of Cu(II) were up to 3.4×10^6 t, accounting for more than 7% of heavy metals in contaminated soils [1]. Heavy metals with refractory and long-term retention. Therefore, it is important to find a proper way to purify polluted water and repair contaminated soil. Among various treatment technologies, the adsorption technology has obvious advantages for its low cost, easy operation and efficiency [2,3]. For example, Shen et al. [4] used tannin modified aminated silica as an adsorbent to efficiently remove light rare earth ions in aqueous solution [4]; biochar from *Alternanthera philoxeroides* could remove Pb(II) efficiently [5].

Biochar refers to the C rich product produced during the pyrolysis of common organic residues such as wood, animal wastes, crop residues, municipal waste, and its application as in situ heavy metal immobilization has received extensive attention in recent years [6–13]. Biochar was evaluated as a potential adsorbent to efficiently reduce concentration of Cu(II) in metal-contaminated water [14]. Xu et al. [15] reported that the dairy-manure biochar was effective for sorbing Cu. Although biochar has stable properties, it may still undergo slow changes in the environment. In soils, biochar is likely to experience a range of chemical reactions and physical processes that will lead to the changes of its properties with time [16–18]. The study found that a series of surface of changes of the biochar during the aging process may occur [19]. Surface changes may also affect the adsorption of heavy metal ions during the aging process [20]. Therefore, the study of the effect of biochar aging process

---

* Corresponding author.

to the adsorption behavior of a heavy metal, copper, has important significance. The aging experiment simulates the process of drying and wetting the biochar in the environment, which require an easy experimental condition and has a strong implementation.

Besides, peanut and cotton planting area nearly 7,000 acres in China. A lot of straw was burned directly which led to the waste of resources and environmental pollution. The application of biochar provides a new idea for the utilization of biomass resources as well as the solution of environmental problems in China. In this work, we examined the effects of dry-wet aging on the physical and chemical properties of biochar. The adsorptions of fresh biochar and aged biochar on Cu(II) were studied.

2. Materials and methods

2.1. Materials

The soil was collected from the surface layer (10–20 cm) of an agricultural area which is located at Rizhao, Shandong Province (119°31′N, 35°26′E). The soil samples were air-dried and ground to pass a 0.830-mm sieve. These basic properties of the soils are listed in Table 1.

Two kinds of biochar were used in the experiments. The first biochar was derived from cotton straws and the second from peanut straws. The crop straws were collected from local farmland at Rizhao. After drying at 100°C to constant weight, the crop straws were put into a muffle furnace (KSY-12D-16, Wuhan, China), heated to 500°C and maintained for 2 h under O_2-limited condition. The crop straws were dried to constant weight at 100°C and pyrolyzed at 500°C for 2 h under nitrogen atmosphere.

Pyrolysis yield was calculated according to GB/T 17664-1999 (Wood charcoal and test method of wood charcoal). Ash content was calculated according to GB/T12496.3-1999 (Test methods of wooden activated carbon—Determination of ash content). The pH of the biochar was measured according to GB/T12496.7-1999 (Test methods of wooden activated carbon—Determination of pH). The elemental C, H, O and N contents were determined with elemental analyzer. The specific surface area was measured using a surface analyzer. Biochar samples (CB, CDB, PB and PDB) in KBr wafers (0.5%) were prepared for Fourier transform infrared spectrometer (FTIR) measurements. The FTIR spectra were recorded in the 4,000–500/cm region by a Nicolet FTIR spectra photometer (model 7600, Thermo Fisher Scientific, USA) with a resolution of 4.0/cm. The pore structure of biochar was observed by scanning electron microscope.

Table 1
Basic properties of the soil

Soil sample	Farmland soil
pH	6.06 ± 0.03
Organic matter (g·kg^{-1})	10.9 ± 2.4
Available Fe (mg·kg^{-1})	68.7 ± 15.7
Available Mn (mg·kg^{-1})	30.1 ± 9.2
Total C (mg·kg^{-1})	18.3

3. Aging experiment

By using the experiments of other researchers as reference [21,22], the fresh biochar samples were encased in pore size of 0.075 mm nylon net. The packaged biochar samples were mixed in the soil at a ratio of 14 t hm^{-2} and were put into the artificial climate box (ZRQ-400, Shanghai, China) for dry-wet test. Two kinds of biochar were incubated at constant temperature (25°C ± 1°C) at 30% water holding capacity for 20 d. Then, the biochar samples were incubated at constant temperature (25°C ± 1°C) at 90% water holding capacity for 20 d. After 40 d incubation time, the biochar samples were removed and dried at 60°C ± 1°C. The dried biochar samples passed a 0.150-mm sieve. The two kinds of biochar were defined as peanut dry-wet aging biochar (PDB) and cotton dry-wet aging biochar (CDB), respectively.

4. Batch sorption experiments

4.1. Kinetic studies

The adsorption kinetics of Cu(II) on the fresh biochar samples (CB, PB), the aging biochar samples (CDB, PDB), the blank soil and mixed samples of biochar with soil were studied at 25°C. Soil sample (0.4 g) and biochar sample (0.1 g) were added to the glass centrifuge tube with background electrolyte of 40 mL solution of $NaNO_3$ (0.01 mol/L) and the initial pH of the solution was adjusted to 4.0. After that, the solutions of Cu(II) were added to each above liquids and shaken at a constant speed (200 rpm) for a specific period of contact time. The samples were shaken mechanically at different time intervals. After shaking, the samples were separated and the concentration of Cu(II) in the residual solutions were measured by atomic spectrophotometer. The adsorption amount was calculated by Eq. (1):

$$q_t = \frac{\left(C_0 - C_t\right) \times V}{M} \tag{1}$$

where q_t is the amount (mg/g) of Cu(II) adsorbed at time t (mg/g), C_0 and C_t are the initial and at time t (min) concentrations of Cu(II) in solution, respectively (mol/dm^3). V is the volume of solution (dm^3), and M is the adsorbents weight (g).

In order to explore the possible controlling steps and to elucidate the adsorption mechanism, Lagergren kinetic equation, pseudo-first-order kinetic equation (Eq. (2)) and pseudo-second-order kinetic equation (Eq. (3)) were used to describe the process of the adsorption:

$$\ln\left(q_e - q_t\right) = \ln q_e - k_1 t,\ q_t = q_e\left(1 - e^{-k_1 x}\right) \tag{2}$$

$$t / q_t = \left(1 / k_2 q_e^{\ 2}\right) + \left(1 / q_e\right)t \tag{3}$$

where q_e is the equilibrium adsorption capacity (mg/g), q_t is the amount (mg/g) of heavy metal adsorbed at t (min), k_1 is the rate constant of the pseudo-first-order adsorption (L/h), k_2 is the pseudo-second-order rate constant (g/mg/h).

4.2. Effect of initial concentration of Cu(II)

Soil sample (0.4 g) and biochar sample (0.1 g) were added to the Cu(II) solutions ranging from 80 to 350 mg/L with a background solution of 0.01 mol/L $NaNO_3$. After shaking in a constant temperature shaker for 48 h, the Cu(II) content in the suspension turbid liquid was measured by atomic spectrophotometer. Adsorption isotherms were expressed as the amount of Cu(II) adsorbed by adsorbents at the equilibrium concentration and fitted according to Langmuir (Eq. (4)) and Freundlich equations (Eq. (5)):

$$\frac{C_e}{q_e} = \frac{1}{b \bullet q_m} + \frac{C_e}{q_m} \tag{4}$$

$$\ln q_e = \ln k_f + n \ln C_e \tag{5}$$

where q_e is the equilibrium adsorption capacity (mg/g), C_e is the concentration (mg/L) at equilibrium, k_f is the adsorption capacity (mg/g), n is the Freundlich constant, q_m is the maximum adsorption (mg/g), b is the adsorption equilibrium constant (L/mg).

4.3. pH dependent

Soil sample (0.4 g) and biochar sample (0.1 g) were added to the solution of 200 mg/L Cu(II) in a background solution of 0.01 mol/L $NaNO_3$. Since Cu(II) in alkaline environment may form part of the precipitation, the initial pH value of the solutions ranged from 2.5 to 6.5. After shaking in a constant temperature shaker for 48 h, the final pH value of the suspension turbid liquid was measured, the Cu(II) content in the filtrate was measured by atomic spectrophotometer and the filtrate was dealt with dense nitric acid.

5. Results and discussion

5.1. Physicochemical properties of biochar

5.1.1. Basic properties of biochar

The basic properties of the fresh biochar samples and the aged biochar samples are listed in Table 2. As the biochar samples aged, the pH values of both types of biochar and the surface area of peanut biochar (PB) decreased, whereas the surface area of cotton biochar (CB) increased. Elemental analysis of the two biochar types showed an increase in both the O/C and (O + N)/C ratios after the aging process, which indicated that the polarities were enhanced [23] and that oxygen-containing groups were introduced onto the biochar surfaces. The O/C ratio of CB increased more than that of PB. This is consistent with a previous study [24]. The increase in the H/C ratio indicated a slight decrease in the degree of aromatization, but these changes were not obvious. The results above showed that the aging process increased the polarities of both PB and CB. Through a comparison of the ash content (6.54%) of CB with that (6.97%) of CDB, we found that ash content increased by 6.57%. A comparison of the ash content of PB and PDB showed a decrease of 25.31%. The ash was primarily composed of alkaline earth metal or alkaline earth metal carbonate, oxides and other components.

5.1.2. Spectroscopic analyses

The spectra of the fresh biochar samples and the aged biochar samples are shown in Fig. 1. The band at 3,400 cm^{-1} was due to the characteristic O–H stretching vibration of a hydroxyl group [25]. The band at 2,980 cm^{-1} was assigned to a characteristic aliphatic C–H stretching vibration [26]. The bands at 1,590, 1,593, 1,599 cm^{-1} were characteristic of C=O stretching vibrations of the aromatic groups [27,28]. The PB and CB showed similar changes in the surface functional groups between the fresh and aged biochar. After aging, the intensity of the band at 3,400 cm^{-1} weakened, indicating that the aging process resulted in a decline in the number hydroxyl groups on the surface. Meanwhile, the band at 2,980 cm^{-1} became more intense and this change showed that the aging process made the increase of aliphatics. Moreover, the band of 1,590–1,593 cm^{-1} became more intense, which implied the increase of aromatic groups.

5.1.3. The surface morphology analysis

The surface morphologies of the fresh biochar samples (CB, PB) and their aged biochar samples (CDB, PDB) are shown in Fig. 2. From the micrographs, we can see that the surface morphology and pore structure were obviously changed after the aging process. The full tubular structure of the biochar was destroyed and became broken pieces of a sheet structure; the degree of fragmentation of PDB was more severe than for CDB. Moreover, after the aging process, the surface smooth degree of the two kinds of biochar decreased.

Table 2
Basic properties of the fresh biochar samples and the aged biochar samples

Sample	Ash (%)	pH	SA ($m^2 g^{-1}$)	Elemental composition						
				C (%)	N (%)	H (%)	O (%)	H/C	O/C	(O + N)/C
CB	6.54	8.43 ± 0.02	2.22	83.29	1.29	2.35	6.53	0.03	0.08	0.09
CDB	6.97	7.89 ± 0.02	2.469	64.99	0.64	3.06	24.34	0.05	0.37	0.38
PB	17.66	9.75 ± 0.05	1.636	60.12	1.85	2.98	17.39	0.05	0.29	0.32
PDB	13.19	8.64 ± 0.04	1.062	60.93	1.31	3.52	21.05	0.06	0.35	0.37

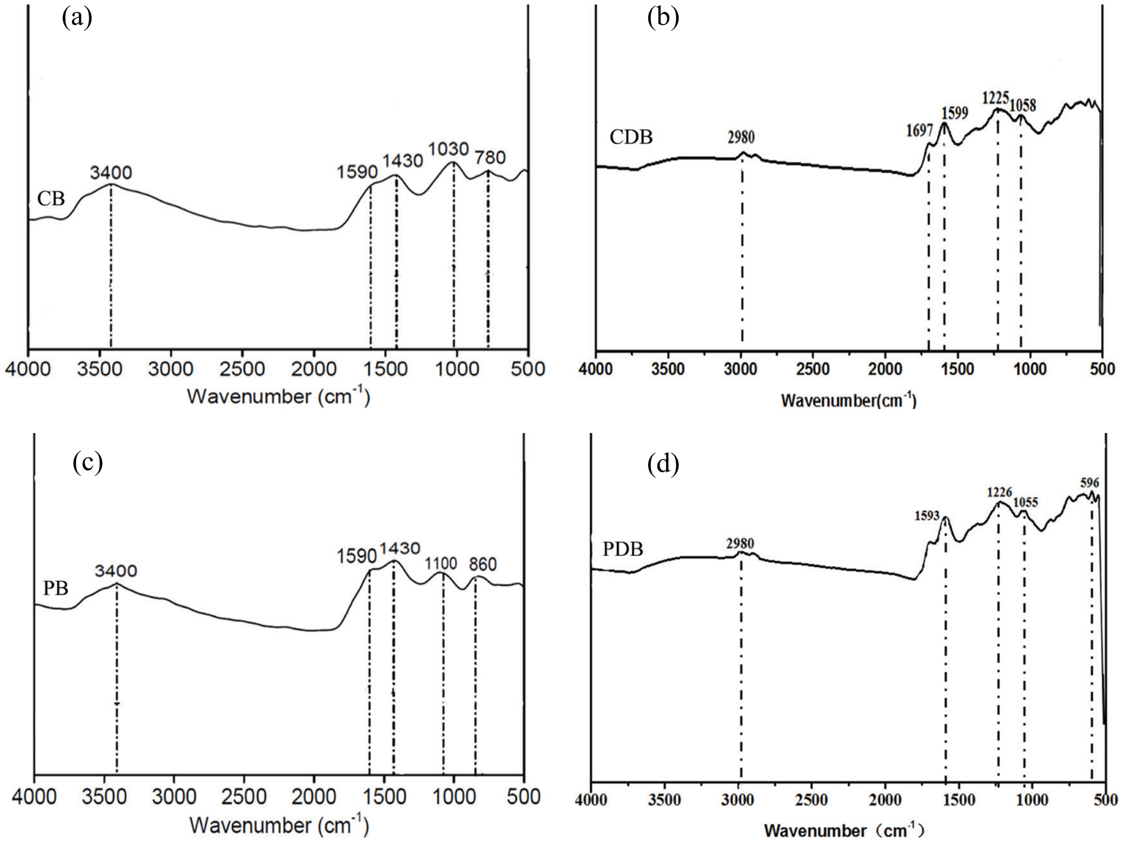

Fig. 1. FTIR spectra of biochar samples and aging biochar samples.

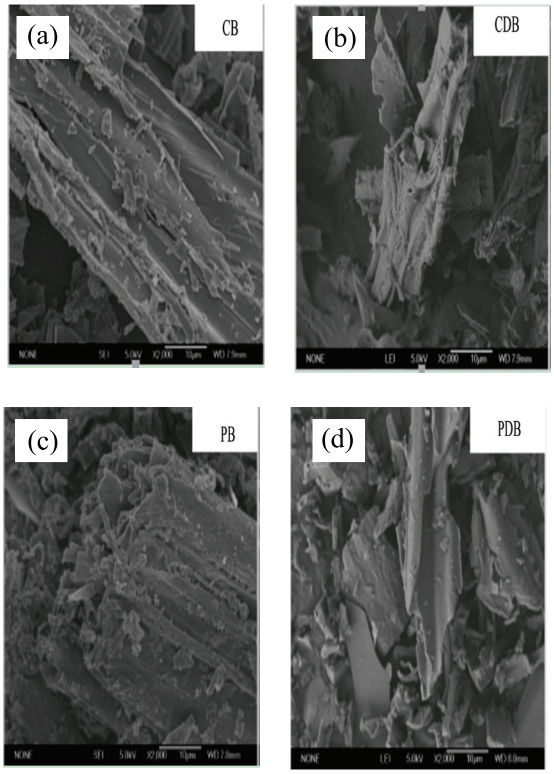

Fig. 2. Scanning electron micrographs of the two kinds of biochar.

5.2. Kinetic studies

Both the first-order kinetic (PF-order) model and second-order kinetic (PS-order) model were fit to the experimental data obtained from batch experiments to elucidate the adsorption mechanism. As shown in Table 3 and Fig. 3, for a comparison of the R^2 values of the PF-order (0.039–0.532) and PS-order (0.995–1.000) models, we found that the PS-order model was more suitable for the fitting of Cu(II) adsorption than the PF-order model. This indicated that the adsorption of Cu(II) was mainly controlled by chemical adsorption [29].

k_2 is the adsorption rate constant reflecting the adsorption rate of biochar on Cu(II). After the aging process, the k_2 values of the various biochar samples (PB, CB and soil biochar mixtures) all decreased. The kinetic data indicated that the aging process led to a decrease of the adsorption rates. The kinetic data also indicated that the rate of chemical reaction and the nature of the adsorption process were determined by the physicochemical characteristics of the adsorbent-like pore structure, specific surface area, etc. [30]. Furthermore, the adsorption of an adsorbate from the aqueous phase involved three steps: film diffusion, intraparticular diffusion and adsorption on the surface of the adsorbent. The slowest of the steps determined the total rate of the adsorption process [20]. After aging, the changes in the specific surface area of PB and CB were inconsistent; however, the pore structures of both types of biochar were destroyed. Therefore, it can be speculated that the destruction of the pore structure was one reason for decreased adsorption. The above analysis suggested that the aging process affected the adsorption rate by changing the biochar pore structure.

Table 3
Pseudo-first-order rate and pseudo-second-order rate constants of adsorption

Samples	PF-order			PS-order		
	q_e (mg/g)	K_1 (h^{-1})	R^2	q_e (mg/g)	k_2 (g/mg/h)	R^2
SCB	7.046	0.320	0.039	8.117	0.011	0.998
SCDB	7.402	0.024	0.367	9.559	0.001	0.995
SPB	16.385	0.089	0.518	17.145	0.013	0.999
SPDB	11.942	0.042	0.498	14.517	0.002	0.999
CB	29.619	0.054	0.179	32.162	0.002	1.000
CDB	36.062	0.005	0.585	40.330	0.000	0.988
PB	78.529	0.074	0.603	84.776	0.001	1.000
PDB	53.423	0.036	0.428	67.609	0.000	0.998
S	4.607	0.532	0.066	4.226	0.012	0.999
SD	4.607	0.532	0.066	4.226	0.012	0.999

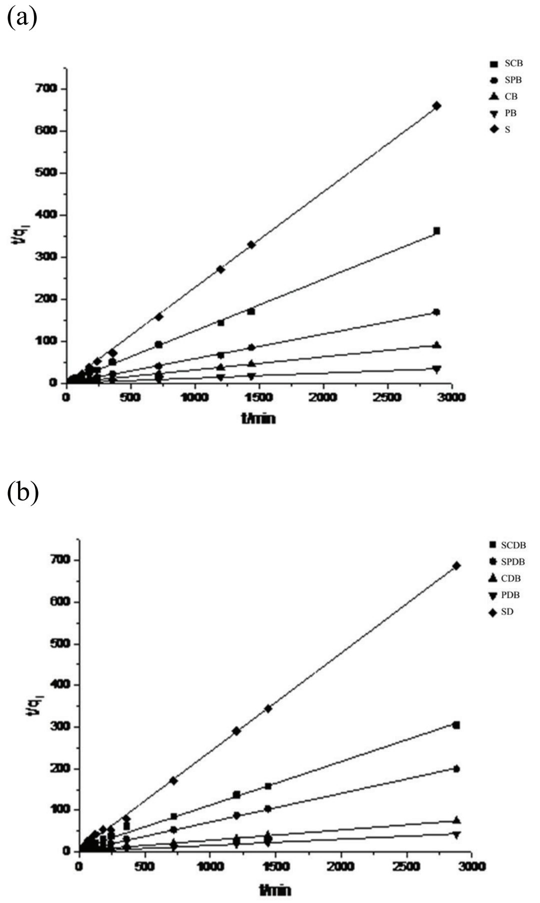

Fig. 3. Effect of contact time on the uptake of Cu(II) by the various soil biochar mixtures.

5.3. Effect of the initial concentration of Cu(II)

The Cu(II) adsorption capacity of the various biochar systems was quantified by applying the non-linear form of the Freundlich and Langmuir equations to the adsorption data. The R^2 values and other coefficients are shown in Table 4. By comparing the R^2 values, the data for adsorption of Cu(II) on the biochar systems fit well with both models but slightly favored the Langmuir adsorption model. The adsorption isotherms are shown in Fig. 4. The values of the maximum adsorption capacities (q_m) are also shown in Table 4. According to the Langmuir adsorption model, q_m followed the order PB > PDB > CDB > CB, SPB > SPDB > SCDB > SCB > S, which indicated that PB had more adsorption sites and the best adsorption effect. In addition, the order of adsorption of biochar samples after mixing with soil did not change. By comparing the Cu(II) adsorption capacity (20.434 mg/g) of CB with that of CDB (80.076 mg/g), we found that q_m was increased by a factor of 2.92. A comparison of the Cu(II) adsorption capacity (150.210 mg/g) of PB with that (81.770 mg/g) of PDB revealed that q_m decreased by 45.56%. These adsorption capacity changes indicated that the aging process may have an impact on the adsorption capacity.

Consistent changes also occurred for the specific surface area. After the aging process, the specific surface area of CB increased and that of PB decreased. A similar phenomenon also occurred in a study by Guo et al. [21]; the adsorption capacity of biochar decreased with a decrease in the specific surface area of the biochar. Therefore, we inferred that the change of specific surface area was one of the reasons for the change of adsorption capacity. Moreover, before and after aging, the adsorptions of separate biochar were better than the adsorptions of the biochar and soil mixture.

5.4. pH dependence

The adsorption capability of the biochar to Cu(II) varied with pH. The effect of pH on the adsorption of Cu(II) in various biochar systems is shown in Fig. 5.

Table 4
Freundlich and Langmuir isothermal fitting results of Cu(II) adsorption

Samples	Langmuir equation			Freundlich equation		
	q_m ($mg\cdot g^{-1}$)	b	R^2	K	n	R^2
SCB	5.854	0.037	1.000	2.407	0.142	0.997
SPB	35.173	0.003	0.967	0.558	0.608	0.945
CB	20.434	0.048	0.996	10.257	0.109	0.992
PB	150.210	0.004	0.964	3.593	0.554	0.939
S	4.053	0.005	0.965	0.136	0.506	0.961
SCDB	16.250	0.005	0.948	0.546	0.505	0.968
SPDB	29.982	0.003	0.983	0.439	0.613	0.989
CDB	80.076	0.003	0.964	1.425	0.588	0.968
PDB	81.770	0.008	0.992	5.203	0.420	0.993
SD	4.053	0.005	0.965	0.136	0.506	0.961

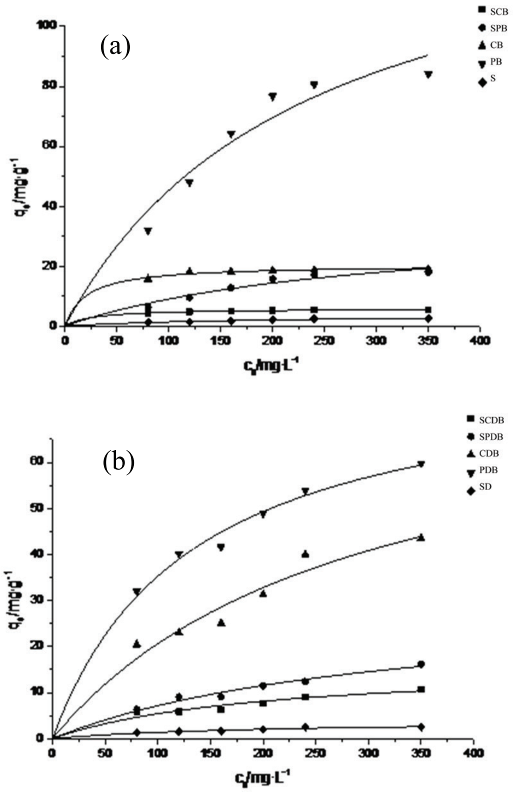

Fig. 4. Adsorption isotherms on Cu(II) by various biochar systems.

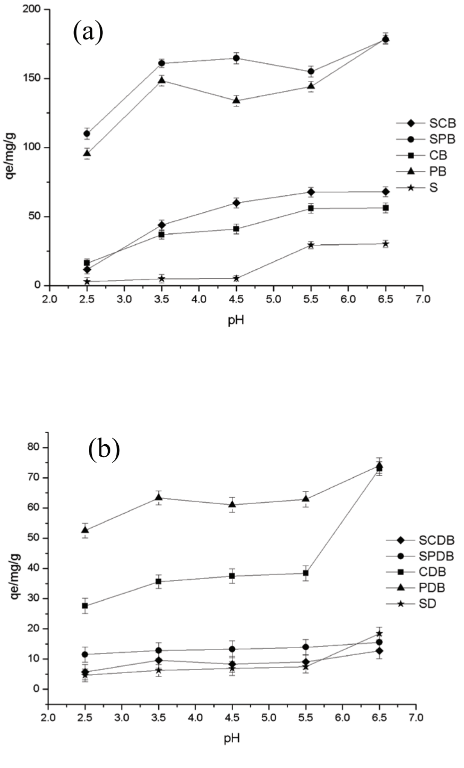

Fig. 5. Effect of pH on the adsorption of Cu(II) in various biochar systems.

The adsorption capacity of various biochar systems increased with the increase of pH value. This was due to increases in the degree of surface functional group dissociation, surface electronegativity and the number of adsorption sites [21]. Moreover, compared with the fresh biochar samples (CB, PB), the adsorption capacity of the aged biochar samples (CDB, PDB) decreased, indicating that the aging process weakened the adsorption capacity of biochar [24]. These observations may be attributed to a decrease of the Cu(II) adsorption sites. As can be seen in Fig. 5, the changes (11.32–16.76 mg/L) in adsorption capacity of CDB and CB were smaller than the changes (42.99–104.97 mg/L) of PB and PDB in terms of adsorption capacity, which can be attributed to the difference (Table 2) in the changes of the specific surface area of the two kinds of biochar after aging. Overall, these downward trends indicated that the change of Cu(II) adsorption capacity was caused by a number of factors.

6. Conclusions

The effects of the dry-wet aging process on the adsorption of Cu(II) were investigated in this study. Based on the experimental results, the following conclusions were made. After the aging process, the adsorption capacity of CB increased, and the adsorption capacity of PB decreased. The number of oxygen-containing functional groups and the O/C ratio increased; the increase of the O/C ratio in CB was higher than that in PB. The effects of aging on the composition of the functional groups on the two types of biochar were similar. However, there was a consistency between the changes of the specific surface area, ash content and adsorption capacity of the biochar samples. The ash contained alkaline substances and oxides; as the ash content increased, the aromatization and surface area of the biochar also increased. The size of the specific area was directly affected by the number of adsorption sites. Based on the above information, we conclude that the changes in ash content and specific surface area are the main factors affecting the Cu(II) adsorption capacity on biochar.

Acknowledgments

This project was supported by the National Natural Science Foundation of China (No. 41471389) and the Natural Science Foundation of Shandong Province (No. ZR2013DM005). Moreover, we express our sincere thanks to Jing Yande, Ju Wenliang and Sun Xiaoxiao for help in setting up and running the experiments.

References

[1] Z.Y. Zhou, Y.P. Fan, M.J. Wang, Heavy metal contamination in vegetables and their control in China, Food. Rev. Int., 16 (2000) 239–255.

[2] I. Ali, V.K. Gupta, Advances in water treatment by adsorption technology, Nat. Protoc., 1 (2006) 2661–2667.

[3] A. Demirbas, Heavy metal adsorption onto agro-based waste materials: a review, J. Hazard. Mater., 157 (2008) 220–229.

[4] Y.Y. Shen, R.L. Yang, Y. Liao, J. Ma, H. Mao, S.L. Zhao, Tannin modified aminated silica as effective absorbents for removal of light rare earth ions in aqueous solution, Desal. Wat. Treat., 57 (2016) 18529–18536.

[5] Y. Yang, Z. Wei, X. Zhang, X. Chen, D. Yue, Q. Yin, L. Xiao, L. Yang, Biochar from *Alternanthera philoxeroides* could remove Pb (II) efficiently, Bioresour. Technol., 171 (2014) 227–232.

[6] B. Chen, M. Yuan, Enhanced sorption of polycyclic aromatic hydrocarbons by soil amended with biochar, J. Soils Sediments, 11 (2011) 62–71.

[7] B. Chen, M. Yuan, L. Qian, Enhanced bioremediation of PAH-contaminated soil by immobilized bacteria with plant residue and biochar as carriers, J. Soils Sediments, 12 (2012) 1350–1359.

[8] A. Downie, P. Munroe, A. Cowie, L.V. Zwieten, D.M.S. Lau, Biochar as a geoengineering climate solution: hazard identification and risk management, Crit. Rev. Environ. Sci. Technol., 42 (2012) 225–250.

[9] G. Fang, J. Gao, C. Liu, D.D. Dionysiou, Y. Wang, D. Zhou, Key role of persistent free radicals in hydrogen peroxide activation by biochar: implications to organic contaminant degradation, Environ. Sci. Technol., 48 (2014) 1902–1910.

[10] J. Lehmann, A handful of carbon, Nature, 447 (2007) 143–144.

[11] L. Qian, B. Chen, Dual role of biochars as adsorbents for aluminum: the effects of oxygen-containing organic components and the scattering of silicate particles, Environ. Sci. Technol., 47 (2013) 8759–8768.

[12] D. Woolf, J.E. Amonette, F.A. Streetperrott, J. Lehmann, S. Joseph, Sustainable biochar to mitigate global climate change, Nat. Commun., 1 (2010) 118–124.

[13] Y. Xu, B. Chen, Organic carbon and inorganic silicon speciation in rice-bran-derived biochars affect its capacity to adsorb cadmium in solution, J. Soils Sediments, 15 (2015) 60–70.

[14] J. Komkiene, E. Baltrenaite, Biochar as adsorbent for removal of heavy metal ions [Cadmium (II), Copper (II), Lead (II), Zinc (II)] from aqueous phase, Int. J. Environ. Sci. Technol., 13 (2016) 471–482.

[15] X. Xu, X. Cao, L. Zhao, H. Wang, H. Yu, B. Gao, Removal of Cu, Zn, and Cd from aqueous solutions by the dairy manure-derived biochar, Environ. Sci. Pollut. Res., 20 (2013) 358–368.

[16] C.H. Cheng, J. Lehmann, M.H. Engelhard, Natural oxidation of black carbon in soils: changes in molecular form and surface charge along a climosequence, Geochim. Cosmochim. Acta, 72 (2008) 1598–1610.

[17] M. Farrell, T.K. Kuhn, L.M. Macdonald, T.M. Maddern, D.V. Murphy, P.A. Hall, B.P. Singh, K. Baumann, E.S. Krull, J.A. Baldock, Microbial utilisation of biochar-derived carbon, Sci. Total. Environ., 465 (2013) 288–297.

[18] S. Kwon, J.J. Pignatello, Effect of natural organic substances on the surface and adsorptive properties of environmental black carbon (char): pseudo-pore blockage by model lipid components and its implications for N_2-Probed surface properties of natural sorbents, Environ. Sci. Technol., 39 (2005) 7932–7939.

[19] C.H. Cheng, J. Lehmann, Ageing of black carbon along a temperature gradient, Chemosphere, 75 (2009) 1021–1027.

[20] D. Kołodyńska, R. Wnętrzak, J.J. Leahy, M.H.B. Hayes, W. Kwapiński, Z. Hubicki, Kinetic and adsorptive characterization of biochar in metal ions removal, Chem. Eng. J., 197 (2012) 295–305.

[21] Y. Guo, W. Tang, J. Wu, Z. Huang, J. Dai, Mechanism of Cu(II) adsorption inhibition on biochar by its aging process, J. Environ. Sci., 26 (2014) 2123–2130.

[22] W. Miao, Ageing Effect of Biochar on Soil Nutrients and Growth of Rice, Shenyang Agricultural University, Shenyang, China, 2014 (In Chinese).

[23] X. Ren, H. Sun, F. Wang, F. Cao, The changes in biochar properties and sorption capacities after being cultured with wheat for 3 months, Chemosphere, 144 (2016) 2257–2263.

[24] L. Qian, B. Chen, Interactions of Aluminum with biochars and oxidized biochars: implications for the biochar aging process, J. Agric. Food Chem., 62 (2014) 373–380.

[25] X.D. Cao, W. Harris, Properties of dairy-manure-derived biochar pertinent to its potential use in remediation, Bioresour. Technol., 101 (2010) 5222–5228.

[26] X. Peng, L.L. Ye, C.H. Wang, H. Zhou, B. Sun, Temperature- and duration-dependent rice straw-derived biochar: characteristics and its effects on soil properties of an Ultisol in southern China, Soil Tillage Res., 112 (2011) 159–166.

[27] Z. Zeng, S.D. Zhang, T.Q. Li, F.L. Zhao, Z.L. He, H.P. Zhao, X.E. Yang, H.L. Wang, J. Zhao, M.T. Rafiq, Sorption of ammonium and phosphate from aqueous solution by biochar derived from phytoremediation plants, J. Zhejiang Univ. Sci. B, 14 (2013) 1152–1161.

[28] L. Zhao, X. Cao, O. Mašek, A. Zimmerman, Heterogeneity of biochar properties as a function of feedstock sources and production temperatures, J. Hazard. Mater., 256–257 (2013) 1–9.

[29] D. Mohan, C.U. Pittman, M. Bricka, F. Smith, B. Yancey, J. Mohammad, P.H. Steele, M.F. Alexandre-Franco, V. Gómez-Serrano, H. Gong, Sorption of arsenic, cadmium, and lead by chars produced from fast pyrolysis of wood and bark during bio-oil production, J. Colloid Interface Sci., 310 (2007) 57–73.

[30] M. Nadeem, A. Mahmood, S.A. Shahid, S.S. Shah, A.M. Khalid, G. Mckay, Sorption of lead from aqueous solution by chemically modified carbon adsorbents, J. Hazard. Mater., 138 (2006) 604–613.